Coxiella burnetii-containing vacuoles interact with host recycling-endosomal proteins Rab11a and Rab35 for vacuolar expansion

Brooke A. Hall[1], Kristen E. Senior[1], Nicolle T. Ocampo[2], and Dhritiman Samanta[1]

[1]Department of Microbiology and Immunology, College of Graduate Studies, Midwestern University, Glendale, AZ, USA

[2]Arizona College of Osteopathic Medicine, Midwestern University, Glendale, AZ, USA

*** Correspondence:**
Dhritiman Samanta
Email: dsaman@midwestern.edu

Keywords: *Coxiella burnetii*, recycling endosomes, Rab11a, Rab35, Intracellular Bacterial Pathogen, confocal microscopy

Abstract

Coxiella burnetii is a gram-negative obligate intracellular bacterium and a zoonotic pathogen that causes human Q fever. Although acute Q fever manifests as atypical pneumonia, chronic infection may lead to life-threatening endocarditis. The lack of effective antibiotics and a licensed vaccine for *Coxiella* in the U.S. warrants further research into *Coxiella* pathogenesis. Within the host cells, *Coxiella* replicates in an acidic phagolysosome-like vacuole termed *Coxiella*-containing vacuole (CCV). Previously, we have shown that the CCV pH is critical for *Coxiella* survival and that the *Coxiella* Type 4B secretion system regulates CCV pH by inhibiting the host endosomal maturation pathway. However, the trafficking pattern of the 'immature' endosomes in *Coxiella*-infected cells remained unclear. Our recent CCV localization screen with host Rab proteins revealed that recycling endosome-associated proteins Rab11a and Rab35 localize to the CCV during infection, suggesting that CCV interacts with host recycling endosomes during maturation. Interestingly, only a subset of CCVs were Rab11a or Rab35-positive at any given time point. A quantitation of Rab11a/Rab35-positive CCVs at 3- and 6-days post-infection (dpi) revealed that at 3 dpi, ~52% of CCVs were positive for Rab11a, whereas only ~39% CCVs were positive for Rab35. This pattern reversed at 6-dpi, when only ~22% of CCVs were positive for Rab11a and ~64% of CCVs were positive for Rab35. These data suggest that the CCV preferentially interacts with Rab11a and Rab35-positive recycling endosomes depending on the stage of maturation. Furthermore, we observed a significant increase in Rab11a and Rab35 fluorescent intensity in *Coxiella*-infected cells compared to mock cells suggesting that *Coxiella* increases the recycling endosome content in infected cells. Finally, a siRNA-mediated knockdown of both Rab11a and Rab35 resulted in significantly smaller CCVs, suggesting that recycling endosomal Rab proteins are essential for CCV expansion. Overall, our data, for the

first time, show that the CCV dynamically interacts with host recycling endosomes for vacuolar expansion and potentially uncovers novel host cell factors essential for *Coxiella* pathogenesis.

1 Introduction

Coxiella burnetii is a highly infectious, zoonotic, bacterial pathogen and the causative agent of human Q (query) fever. In acute cases, Q fever manifests as a flu-like illness, whereas in about 5% of patients, the disease progresses to a chronic stage that often leads to life-threatening endocarditis [1]. The treatment plan for chronic Q fever involves an 18-month-long combined antibiotic therapy and currently, there is no Q fever vaccine licensed in the U.S., presenting challenges in both treating and preventing the disease. Q fever has emerged as a significant public health concern worldwide [2-10].

In the course of a natural infection, *Coxiella* is transmitted through the respiratory route, where alveolar macrophages within the lung parenchyma endocytose the bacteria [11, 12]. Following entry into host cells, *Coxiella* resides in a tight-fitting phagosome that expands and matures over the next 48-72 hours by interacting with the host endocytic pathway [13]. The phagosome maturation pathway involves sequential fusion with the host early and late endosomes, incorporating their respective membrane markers Rab5 and Rab7 [13, 14] and subsequent fusion with lysosomes, acquiring lysosomal markers such as LAMP1 (lysosome-associated membrane glycoprotein-1) and vacuolar ATPase [15-19]. The phagosome-lysosome fusion is a unique event in the *Coxiella* life cycle that generates an acidic phagolysosome-like vacuole with a pH of ~5.2 [20, 21], within which the bacteria multiply. The mature phagosome, termed the *Coxiella*-containing vacuole (CCV), is crucial to *Coxiella* metabolism, replication, and pathogenesis [14, 22, 23].

Previously, using a ratiometric fluorescence-based pH measurement assay, we demonstrated that although the CCV is acidic, further escalation in CCV acidity is bactericidal to *Coxiella* [20] and therefore, *Coxiella* actively regulates CCV acidity in a type 4B secretion system (T4BSS)-dependent manner [21]. Specifically, we showed that *Coxiella* T4BSS inhibits the host endosomal maturation pathway, markedly reducing the number of acidic, mature endosomes and lysosomes available for fusion with the CCV [21]. Since the CCV attains its luminal acidity by fusing with mature endosomes and lysosomes, inhibiting endosomal maturation indirectly aids *Coxiella* in regulating the CCV pH [21]. One notable outcome of *Coxiella* inhibition of endosomal maturation is the increase in mean endosomal pH (pH ~5.2) in the infected cells. Since mature endosomes have a significantly lower pH (~ 4.7), we define the endosomes with an elevated pH as 'immature' endosomes. Because endosomal maturation is crucial to cargo transport and degradation [24], the 'immature' endosomes in *Coxiella*-infected cells may be impaired in these functions and therefore detrimental to host cells. However, the fate and the trafficking pattern of the 'immature' endosomes in *Coxiella*-infected cells remained unclear. In this study, we aim to characterize the endosomal trafficking in *Coxiella*-infected cells by using HeLa cells expressing endosome-specific fluorescent markers analyzed by quantitative confocal microscopy.

The Ras-associated binding (Rab) proteins are the largest family in the Ras superfamily GTPases and are the master regulators of all vesicular trafficking in mammalian cells [25]. Rab proteins localize on the cytosolic surface of endosomes and perform functions like cargo selection and sorting, vesicle transport along microtubules, and vesicle tethering and fusion with target organelles [25]. The human genome encodes more than 60 Rab proteins that are associated with specific endosome populations to regulate their trafficking, sorting, and recycling events. Rab proteins cycle between an active, GTP-bound, membrane-recruited form and an inactive, GDP-bound, cytosolic form to associate and dissociate with specific endosomes [24, 25]. Therefore, the localization of a specific Rab protein provides key information about the trafficking pattern of a population of endosomes in mammalian cells.

To understand the trafficking of the *Coxiella*-generated 'immature' endosomes, we ectopically expressed EGFP-tagged Rab proteins in the infected host cells and analyzed their localization by confocal microscopy. To our surprise, we observed that the CCV, in addition to acquiring Rab5 and Rab7, acquired the recycling endosomal markers Rab11a and Rab35, suggesting that the CCV also interacts with the host recycling endosomes during maturation. Furthermore, we observed an increase in Rab11a and Rab35-positive endosomes in the infected cells, indicating that *Coxiella* enhances the recycling endosome content in the infected cells. Finally, silencing Rab11a and Rab35 using siRNA resulted in significantly smaller CCVs, suggesting that recycling endosomes facilitate CCV expansion. Our study is the first report suggesting a CCV-host recycling endosome interaction indicating the importance of recycling endosomes in the *Coxiella* intracellular life cycle.

2 Materials and methods

2.1 Bacteria and mammalian cells

Coxiella burnetii Nine Mile Phase II (NMII) (Clone 4, RSA 439) and mCherry-expressing *C. burnetii* NMII [26] were grown and stored as previously described [21]. Human cervical epithelial cells (HeLa, ATCC CCL-2) were maintained in Roswell Park Memorial Institute (RPMI) 1640 medium with glutamine (Cat. 10-040-CV, Corning, New York, NY) and 10% fetal bovine serum (FBS; Cat. S11150, R&D Systems, Inc., Minneapolis, MN). The genome equivalents (GE) for the *Coxiella* stocks were determined by qPCR using primers for the *Coxiella burnetii dotA* gene [27]. The multiplicities of infection (MOI) of the bacteria stocks were optimized for HeLa cells and each type of culture vessels to ~1 internalized bacterium per cell at 37℃ and 5% CO_2.

2.2 Preparation of EGFP-tagged Rab plasmids

The plasmids encoding EGFP-tagged Rab proteins were generous gifts from Dr. Mary Weber, University of Iowa [28]. The plasmids were first transformed into competent *E. coli* DH5α (Cat. C2988J, New England Biolabs, Ipswich, MA) and stored at -80˚C. A single colony of the transformed *E. coli* was grown in 5 mL lysogeny broth (LB) containing 50 µg/mL kanamycin or 100 µg/mL carbenicillin overnight, which was then used to inoculate a 150 mL LB culture and incubated overnight. The GeneJET Endo-free Plasmid Maxiprep Kit (Cat. K0861, Thermo Fisher Scientific Baltics UAB, Lithuania) was used to isolate and purify plasmid DNA from bacterial cultures according to the manufacturer's protocol. Plasmids were then concentrated using the MilliporeSigma Amicon Ultra-0.5 Centrifugal Filter Units (Cat. UFC503096, Fisher Scientific, Waltham, MA) and stored at -20˚C until used for cell transfection.

2.3 Transfection and immunofluorescent assay

HeLa cells, grown in RPMI with 10% FBS (hereafter referred to as 10% RPMI), were plated in a 24-well plate ($2x10^4$ cells per well) and simultaneously transfected with 0.4 µg of respective EGFP-Rab plasmids using FuGENE 6 transfection reagent (Cat. E269A, Promega, Madison, WI) per the manufacturer's protocol. At 24 hours post-transfection, the cells were infected with mCherry-*Coxiella* in 250 uL 10% RPMI for 1 h, washed extensively with sterile phosphate-buffered saline (PBS; HyClone, Cat. SH30256.01, Cytiva, Marlborough, MA), and incubated in 10% RPMI at 37˚C. On the day before the indicated time points, cells were trypsinized, counted, and diluted to $1x10^5$ cells/mL. Diluted cells were then plated onto coverslips placed in a separate 24-well plate ($5x10^4$ cells per coverslip) and allowed to adhere overnight. The next day, cells were fixed in 2.5% paraformaldehyde (PFA; Cat. 15710, Electron Microscopy Sciences, Hatfield, PA) for 15 min, washed in PBS, and blocked/permeabilized for 20 min in 1% bovine serum albumin (BSA; Cat.

128 BP9700-100, Fisher BioReagents, Pittsburgh, PA) and 0.1% saponin (Cat. S0019, TCI America,
129 Portland, OR) in PBS. Cells were then incubated in rabbit anti-LAMP1 (1:1000; Cat. PA1-654A,
130 Thermo Fisher Scientific, Waltham, MA) primary antibody for 1h followed by Alexa Fluor secondary
131 antibody (1:1000; Life Technologies) for 1 h to label the CCV. Following washing with PBS,
132 coverslips were mounted using ProLong Gold Antifade Mountant with 4', 6'-diamidino-2
133 phenylindole (DAPI; Cat. P36941, Invitrogen, Carlsbad, CA) and visualized on a Leica Stellaris
134 confocal microscope using a 63x oil immersion objective. Images were processed and analyzed in
135 ImageJ FIJI [29].

136 **2.4 Enumeration of Rab11a/Rab35-positive CCVs**

137 HeLa cells were plated in a 24-well plate and transfected with plasmids encoding EGFP-tagged
138 Rab11a or Rab35 using FuGENE 6 transfection reagent according to the manufacturer's protocol. At
139 24 hours post-transfection, the cells were infected with mCherry-*Coxiella* in 250 µL 10% RPMI for 1
140 h, washed in PBS, and incubated in 10% RPMI. On the day before the indicated time points, cells
141 were trypsinized, diluted to $1x10^5$ cells/mL, and plated onto coverslips in a 24-well plate ($5x10^4$ cells
142 per coverslip). The next day, the cells were subjected to immunofluorescent assay (IFA) where they
143 were fixed with 2.5% PFA for 15 min and blocked/permeabilized with 1% BSA in PBS with 0.1%
144 saponin for 20 min. Cells were then incubated in rabbit anti-LAMP1 (1:1000; Cat. PA1-654A,
145 Thermo Fisher) primary antibody for 1 h followed by Alexa Fluor 647 goat anti-rabbit secondary
146 antibody (1:1000; Cat. A21245, Invitrogen) for 1 h to label the CCVs. Following washing with PBS,
147 the coverslips were mounted with ProLong Gold Antifade Mountant with DAPI. The cells were
148 visualized with a Leica Stellaris confocal microscope using a 63x oil immersion objective and images
149 were imported and analyzed in ImageJ FIJI. A Rab-LAMP1 colocalization at the CCV membrane
150 was considered positive for Rab trafficking to the CCV. Approximately 100 CCVs were scored for
151 Rab11a and Rab35 localization and the percentage of Rab11a- and Rab35-positive CCVs were
152 determined. The statistical difference in the percentage of Rab11a and Rab35-positive CCVs at each
153 time-point was determined by Welch's t-test from three independent experiments (N=3).

154 **2.5 Quantification of Rab11a and Rab35 content in *Coxiella*-infected cells**

155 HeLa cells were either mock-infected or infected with mCherry-*Coxiella* in 24-well plates ($2.5x10^4$
156 cells per well; two wells per condition) for 1 h, washed extensively with PBS, and incubated in 10%
157 RPMI. For 3-day experiments, the cells were trypsinized at 2 dpi, diluted to $1x10^5$ cells/mL, and
158 replated onto coverslips in a new 24-well plate ($5x10^4$ cells per coverslip). At 3 dpi, cells were fixed
159 with 2.5% PFA for 15 min and washed thoroughly with PBS. For 6-day experiments, cells were
160 trypsinized, diluted, and replated first at 3 dpi and again at 5 dpi ($5x10^4$ cells per coverslip). Next day,
161 cells were fixed with 2.5% PFA and washed thoroughly with PBS. For both 3-day and 6-day
162 experiments, following fixation, the cells were blocked/permeabilized with 1% BSA in PBS with
163 0.1% saponin for 20 min. Cells were then incubated overnight at 4°C in rabbit anti-Rab35 (1:100;
164 Cat. 11329-2-AP, Proteintech, Rosemont, IL) or for 1 h at room temperature (RT) in rabbit anti-
165 Rab11a (1:500; Cat. 20229-1-AP, Proteintech) primary antibody. The coverslips were washed with
166 PBS and then incubated in Alexa Fluor 488 goat anti-rabbit (1:1000; Cat. A11034, Invitrogen)
167 secondary antibody for 1 h at RT. Upon washing with PBS, the coverslips were mounted using
168 ProLong Gold with DAPI. Cells were visualized with a Leica Stellaris confocal microscope using a
169 63x oil immersion objective. To quantify Rab content from mock and WT-infected cells, identically
170 captured and processed images were imported into ImageJ FIJI and the total fluorescent intensity of
171 Rab11a or Rab35 was measured and normalized to cell area. At least 25 cells were analyzed per

condition in each of three independent experiments (N=3). The statistical difference in Rab11a and Rab35 intensities between mock and *Coxiella*-infected cells was measured by Welch's t-test.

2.6 RNA interference and immunoblotting

HeLa cells (10^5 cells per well, 6-well plate) were reverse transfected with 50 nM small-interfering RNA (siRNA) SMARTpools specific for human Rab11a (ON-TARGETplus, Cat. L-004726-00-0005, Dharmacon Inc., Horizon Discovery Ltd., Lafayette, CO), Rab35 (ON-TARGETplus, Cat. L-009781-00-0005, Dharmacon Inc.), or a non-targeting (NT) control (Cat. D-001810-10-05, Dharmacon Inc.) using DharmaFECT-1 transfection reagent (Cat. T-2001-01, Dharmacon Inc.) in RPMI with 5% FBS according to the manufacturer's protocol. At 48 h post-transfection, cells were infected with mCherry-*Coxiella* for 1 h at 37°C. Following washing with PBS, cells were harvested by trypsinization and subjected to a second round of siRNA transfection in a 24-well plate ($2.5x10^4$ cells per well). On the day before the indicated time points, cells were trypsinized, resuspended to $1x10^5$ cells/mL, and either replated onto coverslips ($2.5x10^4$ cells per coverslip) or into another 24-well plate without coverslips. The next day, the cells on coverslips were fixed with 2.5% PFA and subjected to immunofluorescent assay with rabbit anti-LAMP1 primary and Alexa Fluor 488 secondary antibodies to label the CCVs. Concurrently, mock-infected cells from the second 24-well plate were lysed with RIPA lysis buffer (Cat. 89900, Thermo Fisher) supplemented with HALT protease inhibitor (Cat. 87786, Thermo Fisher) on ice. The soluble fraction from the cell lysates were collected and protein concentrations were determined using the Pierce Rapid Gold BCA kit (Cat. A53226, Thermo Fisher). To confirm Rab11a and Rab35 silencing, 10 µg of total protein for both NT and Rab siRNA-transfected samples were resolved in 4-20% gradient SDS-PAGE (Mini-PROTEAN Gel, Cat. 4561094, Bio-Rad Laboratories, Hercules, CA) and subsequently transferred to a PVDF membrane for immunoblotting (Immun-Blot PVDF Membrane, Cat. 1620174, Bio-Rad). After blocking in Bio-Rad EveryBlot buffer (Cat. 12010020, Bio-Rad) for 5 min, the membranes were then probed separately using rabbit anti-Rab11a (Cat. 20229-1-AP, Proteintech), rabbit anti-Rab35 (Cat. 11329-2-AP, Proteintech), and anti-β-tubulin (BT7R) (HRP-conjugated loading control; Cat. MA5-16308-HRP, Invitrogen) antibodies in 1% BSA in PBS. After washing, the membranes were incubated with horseradish peroxidase-conjugated goat anti-rabbit (1:1000; Cat. 31460, Thermo Fisher) secondary antibody in EveryBlot blocking buffer, and developed using enhanced chemiluminescence (ECL) reagent (Cat. 170-5060, Bio-Rad).

2.7 Measurement of CCV area

HeLa cells were reverse-transfected with NT control, Rab11a, or Rab35-specific siRNAs as described above, and at 48 h post-transfection, were infected with mCherry-*Coxiella* for 1 h. Upon washing with PBS, cells were subjected to a second round of siRNA transfection as described above. On the day before the indicated time points, cells were trypsinized, resuspended to $1x10^5$ cells/mL, and replated onto coverslips ($2.5x10^4$ cells/coverslip). The next day, the coverslips were fixed with 2.5% PFA and cells were immunostained with rabbit anti-LAMP1 primary antibody and Alexa Fluor secondary antibody to label the CCVs. Mounted coverslips were visualized using a Keyence BZ-X710 fluorescent microscope. Images of individual CCVs were captured and processed identically between conditions, and the CCV areas from exported images were measured in ImageJ FIJI. A 20 µm scale bar placed on a representative image for each sample was used for setting the scale in ImageJ. CCV areas were expressed as pixels and plotted using GraphPad Prism. At least 25 CCVs were measured per condition for each of the three independent experiments (N=3). The statistical differences in CCV areas between non-targeting and Rab11a/Rab35-specific siRNA-transfected cells were measured by Welch's t-test.

217 **2.8 Data analyses**

218 Fluorescent and confocal images were processed and analyzed in ImageJ FIJI software [29]. All
219 statistical analyses were performed using unpaired t-test with Welch's correction (Welch's t-test)
220 using GraphPad Prism (GraphPad, La Jolla, CA). A p-value < 0.05 was considered significant. Data
221 are plotted as mean ± standard error of mean (SEM).

222 **3 Results**

223 **3.1 Recycling endosomal markers Rab11a and Rab35 localize to the CCV during infection**

224 We previously observed that *Coxiella* actively regulates the CCV acidity by inhibiting host
225 endosomal maturation in a T4BSS-dependent manner [21]. However, by impeding endosomal
226 maturation, *Coxiella* gives rise to population of 'immature' endosomes with a higher mean pH
227 compared to mature endosomes. As the immature endosomes may be impaired in cargo trafficking
228 and degradation, they may be detrimental to the host cells. However, whether *Coxiella* manipulates
229 the trafficking of the 'immature' endosomes in the infected cells has not been clear. Since Rab
230 proteins are the master regulators of endocytic trafficking, we hypothesized that *Coxiella* manipulates
231 one or more Rab proteins to modulate endosomal trafficking in the infected cells. To test this, we
232 screened 13 major Rab proteins in *Coxiella*-infected cells for their interaction with the CCV.
233 Plasmids encoding EGFP-tagged Rab proteins (Table 1; a gift from Dr. Mary Weber, University of
234 Iowa) were maxiprepped from *E. coli* culture and stored in endotoxin free elution buffer. HeLa cells
235 were transfected with the EGFP-Rab plasmids and infected with mCherry-*Coxiella*. At 3 dpi, the
236 cells were immunostained with LAMP1 primary antibody to label the CCVs. The cells were then
237 visualized with a Leica Stellaris confocal microscope where 488 and 647 nm lasers were used for
238 imaging the Rab proteins and LAMP1, respectively. Images were processed and analyzed in ImageJ
239 FIJI and a Rab-LAMP1 colocalization at the CCV was considered positive for Rab trafficking to the
240 CCV. EGFP tagged-Rab5 and Rab7 were included as positive controls in the screen as Rab5 and
241 Rab7 are known to localize to the CCV during infection [30, 31]. As expected, all CCVs were
242 positive for Rab5, Rab7, and LAMP1. In addition to that, we interestingly observed that some CCVs
243 were also positive for Rab11a and Rab35 as evidenced by their colocalization with LAMP1 at the
244 CCV membrane (Figure 1). Both Rab11a and Rab35 are associated with host recycling endosomes,
245 where they regulate the 'slow' and 'fast' endosomal recycling pathways, respectively [32-34].
246 Therefore, these data suggest that, in addition to interacting with early endosomes, late endosomes,
247 and lysosomes, at least a subset of CCVs also interacts with the host recycling endosomes in both the
248 'slow' and the 'fast' recycling pathways. A CCV area comparison between the Rab11a/Rab35-
249 positive and the negative CCVs showed no significant difference in areas between the positive and
250 the negative CCVs (data not shown). Moreover, *Coxiella* colonies appeared unaffected by the
251 presence of Rab11a and Rab35 at the CCV. This study is the first report suggesting that the CCV
252 interacts with host recycling endosomes and acquires recycling endosomal markers during
253 maturation.

254 **Table 1. EGFP-tagged Rab proteins used in this study**

Rab proteins	Cellular localization	Membrane traffic function	References	Traffics to CCV
Rab1a	ER, Golgi	ER to Golgi	[35]	No
Rab4a	Early endosome	Protein recycling, transport to PM	[36]	No
Rab5	Early endosome, PM	Early endosome fusion	[37]	Yes

Rab6a	Golgi	Endosome to Golgi, intra-Golgi transport	[38]	No
Rab7	Late endosomes, lysosomes	Late endosome to lysosome	[37]	Yes
Rab8	Cell membrane, primary cilia	Exocytosis, TGN to PM	[39]	No
Rab9	Late endosomes, Golgi	Endosome to TGN	[40]	No
Rab11a	Recycling endosomes, Golgi	TGN/RE to PM	[41]	
Rab14	Golgi, early endosomes	TGN/RE to PM	[42]	No
Rab18	Golgi, lipid droplets	Lipid droplet formation	[43]	No
Rab33	Golgi	Autophagosome formation	[44]	No
Rab34	Golgi	Intra-Golgi transport	[45]	No
Rab35	Recycling endosomes, PM	RE to PM	[46]	Yes

ER – Endoplasmic reticulum; PM – plasma membrane; TGN – Trans-Golgi Network; RE – Recycling endosomes

3.2 CCV-Rab11a and CCV-Rab35 interactions are dynamic and temporally regulated

In our Rab localization screen, we interestingly observed that only a subset of the CCVs were positive for Rab11a or Rab35 at a given time-point. This led us to hypothesize that the interaction between the CCV and Rab11a/Rab35 are dynamic in nature. To test this, we quantified the percentage of Rab11a- and Rab35-positive CCVs in a population of *Coxiella*-infected HeLa cells at 3 and 6 dpi. Rab11a- or Rab35-positive and negative CCVs were identified in ImageJ FIJI by a colocalization of Rab and LAMP1 at the CCV membrane, as described above (Figure 2A). Our quantitation data revealed that at 3 dpi, ~52% of CCVs were positive for Rab11a, whereas only ~39% of CCVs were positive for Rab35 (Fig. 2B-C). Interestingly this pattern reversed at 6 dpi, when only ~22% of CCVs were positive for Rab11 and ~64% of CCVs were positive for Rab35 (Fig. 2B-C). Together, these data suggest that, while CCVs preferentially interact with the Rab11a-positive endosomes at 3pi, at 6 dpi, the preferential interaction shifts towards the Rab35-positive endosomes. Therefore, our data indicate that Rab11a and Rab35 interaction with the CCV are dynamic and varies depending on the stage of infection.

3.3 *Coxiella* infection leads to increased recycling endosome content in infected cells

Our observation that *Coxiella* interacts with two different populations of recycling endosomes in the host cells led us to hypothesize that *Coxiella* manipulates host recycling endosomes during infection. To test this hypothesis, we quantitated the total cellular Rab11a and Rab35 content in mock and *Coxiella*-infected HeLa cells by immunofluorescent assay with anti-Rab11a or anti-Rab35 antibody. EGFP-Rab11 or EGFP-Rab35 transfected HeLa cells were not used in this experiment because of potential differences in ectopic expression level of Rab proteins between individual cells. Mock and *Coxiella*-infected HeLa cells were immunostained using anti-Rab11a or anti-Rab35 antibodies at 3 and 6 dpi and identically captured images were analyzed in ImageJ FIJI. The total fluorescent intensity of Rab11 or Rab35 was measured from mock and *Coxiella*-infected cells normalized to cell area and were considered indicative of total recycling endosome content in each cell. Our data revealed a ~19% increase in Rab11a fluorescent intensity ($p < 0.0001$; Figures 3A, B) and a ~27% increase in Rab35 fluorescent intensity in infected cells compared to mock at 3 dpi ($p < 0.0001$; Figures 4A, B). However, to our surprise, we did not observe any difference in Rab11a or Rab35

fluorescent intensities between mock and *Coxiella*-infected cells at 6 dpi (Figures 3C, 4C). These data suggest that *Coxiella* increases the recycling endosome content in infected host cells at 3 dpi, but not at 6 dpi.

3.4 Rab11a and Rab35 silencing inhibits CCV expansion

Based on our observation that the CCV dynamically interacts with recycling endosome-associated Rab11a and Rab35, and that *Coxiella* increases the recycling endosome content of infected cells, we hypothesized that Rab11a and Rab35 positively affects CCV maturation. To test this, we examined CCV expansion in Rab11a or Rab35 knockdown HeLa cells compared to a non-targeting (NT) control using our dual-hit siRNA knockdown protocol described previously (Figure 5A) [21]. Since CCV interaction with Rab11a is higher at 3 dpi, and that with Rab35 is higher at 6 dpi, we measured the CCV areas in Rab11a and Rab35 knockdown cells at 3 dpi and 6 dpi, respectively, to detect maximum effect of the respective knockdowns. Immunoblotting with cell lysates from NT, siRab11a, and siRab35-transfected cells revealed significant depletion of both Rab11a (Figure 5B) and Rab35 (Figure 5C) at 3 and 6 dpi, respectively. The CCV area measurement data revealed a ~45% reduction in CCV area in Rab11a knockdown cells compared to NT ($p<0.0001$) at 3 dpi (Figure 5D), and a ~28% reduction in CCV area in Rab35 knockdown cells ($p<0.0001$) at 6 dpi (Figure 5E). These data suggest that both Rab11a and Rab35 positively affect CCV expansion at 3 and 6 dpi, respectively, indicating that host recycling endosomes are essential for CCV maturation.

4 Discussion

We previously established that *Coxiella* T4BSS inhibits host endosomal maturation for bacterial survival and pathogenesis. However, in the process, *Coxiella* generates a population of 'immature' endosomes with an elevated mean pH relative to mature endosomes. To generate a comprehensive understanding of endosomal trafficking in the *Coxiella*-infected cells, we screened 13 well-studied Rab proteins to assess their localization in *Coxiella*-infected cells. We discovered that Rab11a and Rab35, the molecular markers of recycling endosomes, localize to the CCV, although only a subset of CCVs were found positive for Rab11a or Rab35 at a given time point. Our data also revealed that *Coxiella* increases the recycling endosome content of the infected cells at 3 dpi, and Rab11a and Rab35 knockdown resulted in significantly smaller CCVs at 3 and 6 dpi, respectively, suggesting that host recycling endosomes are essential for CCV expansion.

Mammalian endosomal trafficking can be broadly classified into degradative and recycling pathways [47]. While the degradative pathway traffics the cargo through early and late endosomes and finally delivers it to lysosomes for degradation, the recycling pathway sorts and re-exports essential membrane components including receptors, carrier molecules, and cell adhesion molecules that have been internalized [33]. For the first time, we present findings suggesting an interaction between the CCV and the host recycling endosomes. This intriguing observation implies that the CCV not only engages with the host endocytic degradative endosomes but also with recycling endosomes, potentially incorporating their contents and membranes during maturation. Mammalian cells exhibit two simultaneous pathways for cargo recycling namely the 'fast' and the 'slow' recycling pathways [48]. In the 'fast' pathway, the internalized cargo is directly transported back to the plasma membrane from early endosomes. However, the 'slow' pathway first traffics the cargo to a perinuclear vesicle known as the endocytic recycling compartment (ERC), within which, the cargo is sorted and then redirected to the plasma membrane via recycling endosomes [33, 49]. Rab35 predominantly regulates the 'fast' recycling pathway [32, 34], while Rab11a serves as a major regulator of the 'slow' pathway [33, 34, 50]. Therefore, our data suggest that the CCV interacts with both the 'fast' and the 'slow' recycling pathways during maturation. Moreover, our observation that

330 Rab11a localizes to the CCVs significantly more at 3 dpi whereas Rab35 is more prevalent at CCVs
331 at 6 dpi suggest a preference for interaction with the 'slow' recycling pathway during the early stages
332 of maturation and a shift towards a preferential interaction with the 'fast' recycling pathway as the
333 CCV matures further.
334 While the significance of the interactions between CCV and the host recycling endosomes
335 remains uncertain, multiple studies propose that similar interactions with intracellular bacterial
336 vacuoles play a crucial role in providing nutrients to the vacuole or in ensuring vacuolar stability. For
337 example, *Chlamydophila pneumoniae*-containing inclusions recruit the mammalian Rab11/Rab14
338 adapter protein Fip2, facilitating the early-stage recruitment of Rab11/14 to the inclusion membrane
339 during infection [51, 52]. Rab11/14 positive recycling endosomes trafficked nutrients, such as
340 transferrin to the proximity of *C. pneumoniae* inclusion, although whether transferrin is delivered
341 into the inclusion lumen remained unclear [53-55]. Indeed, a recent study with fluorescent transferrin
342 (Tf488) revealed that in *Coxiella*-infected HeLa cells, Tf488-containing vesicles also trafficked to the
343 proximity of CCVs [56]. Moreover, Rab11-positive recycling endosomes trafficked transferrin in
344 K562 cells [50]. Therefore, it is possible that recycling endosomes traffic transferrin to the CCV
345 aiding in its maturation. Further experimentation is needed to examine this intriguing hypothesis.
346 Another possible benefit of intracellular pathogens subverting recycling endosomes is to augment
347 vacuole stability. For example, *Chlamydia trachomatis* inclusion protein CT229 interacts with Rab35
348 to maintain the inclusion integrity [28], and *Legionella pneumophila*-containing vacuoles (LCV)
349 acquire Rab11 and Rab35 for stability [57]. It is possible that Rab11 and Rab35 plays a critical role in
350 maintaining CCV stability. However, we did not observe a disintegration of CCV in Rab11a and
351 Rab35 knockdown HeLa cells, raising a possibility that *Coxiella* employes redundant mechanisms to
352 maintain CCV stability.
353 As mentioned before, we observed that only a subset of CCVs are positive for Rab11a or
354 Rab35 at a given time point, and the proportion of Rab11a- and Rab35-positive CCVs in a population
355 of infected cells vary over time. previous studies including ours have only observed stable fusion
356 events between the CCV and host endosomes and lysosomes [14, 20, 21, 58]. The dynamic nature of
357 CCV-Rab11a/Rab35 interactions could be a result of two possibilities: first, only a subset of CCVs
358 preferentially interacts with the recycling endosomes at a given time point and the number of
359 preferred CCVs interacting with a particular Rab protein varies depending on the stage of infection,
360 and second, it is possible that the recycling endosomes make transient contact with the CCVs in a
361 'kiss-and-run' manner [59], to release their content into the CCV and/or to receive recyclable cargo
362 from the CCV and then dissociate. However, further experimentation is required to test these
363 hypotheses and could be an intriguing area of future investigation.
364 Our observation that *Coxiella* infection led to an increased recycling endosome content at 3
365 dpi builds upon the previous observation that *Coxiella* expands the endosomal compartment in
366 infected cells [56]. It is possible that increased number of recycling endosomes accumulate more
367 Tf488 in *Coxiella*-infected cells observed in that study [56]. Interestingly, in our study, we did not
368 observe an increase in the recycling endosome content at 6 dpi. This may be a result of an already
369 low number of endosomes in the *Coxiella*-infected cells at 6 dpi [21]. Nonetheless, these data, taken
370 together with our previous data indicate that *Coxiella* has a dual effect on host endosomes: while it
371 reduces the number of mature endosomes in infected cells [21], *Coxiella* simultaneously elevates the
372 number of recycling endosomes during infection. While the full characterization of these regulations
373 requires further testing, we propose a model that *Coxiella* reroutes the 'immature' endosomes from
374 the degradative pathway into the recycling pathway, potentially protecting the host cell from the
375 detriments of the 'immature' endosomes.
376 Our siRNA-mediated knockdown experiments revealed that Rab11a and Rab35 are essential
377 for CCV expansion at 3 and 6 dpi, respectively. A recent study with Rab11a knockout HeLa cells
378 revealed that Rab11a deficiency increases the number of late endosomes and lysosomes within the

379 cells [60]. It is possible that in our experiments, Rab11a knockdown led to an increased number of
380 lysosomes that is detrimental to CCV acidity and *Coxiella* growth. Future research analyzing the
381 lysosomal pH and enzyme activity in *Coxiella*-infected, Rab11a/Rab35 knockdown cells will help
382 further characterize the CCV-recycling endosome interactions.
383 Overall, our data revealed novel host-*Coxiella* interactions that appear to be beneficial for
384 CCV maturation. Future research into characterizing the role of Rab11a and Rab35 in *Coxiella*
385 pathogenesis, and the molecular mechanisms of *Coxiella* enhancement of recycling endosome
386 content will potentially identify novel therapeutic targets for *Coxiella*.

387 **5 Acknowledgments**

388 We thank Stacey Gilk (University of Nebraska Medical Center) for providing the parental HeLa cells
389 and mCherry-*Coxiella burnetii*. We are also thankful to Mary Weber (University of Iowa) for
390 providing the EGFP-tagged Rab plasmids. We thank Manan Damani (Midwestern University) for
391 assistance with confocal and fluorescent microscopy. We also thanks Vijitha Kantety and Ruthvik
392 Gundala for helpful suggestions.

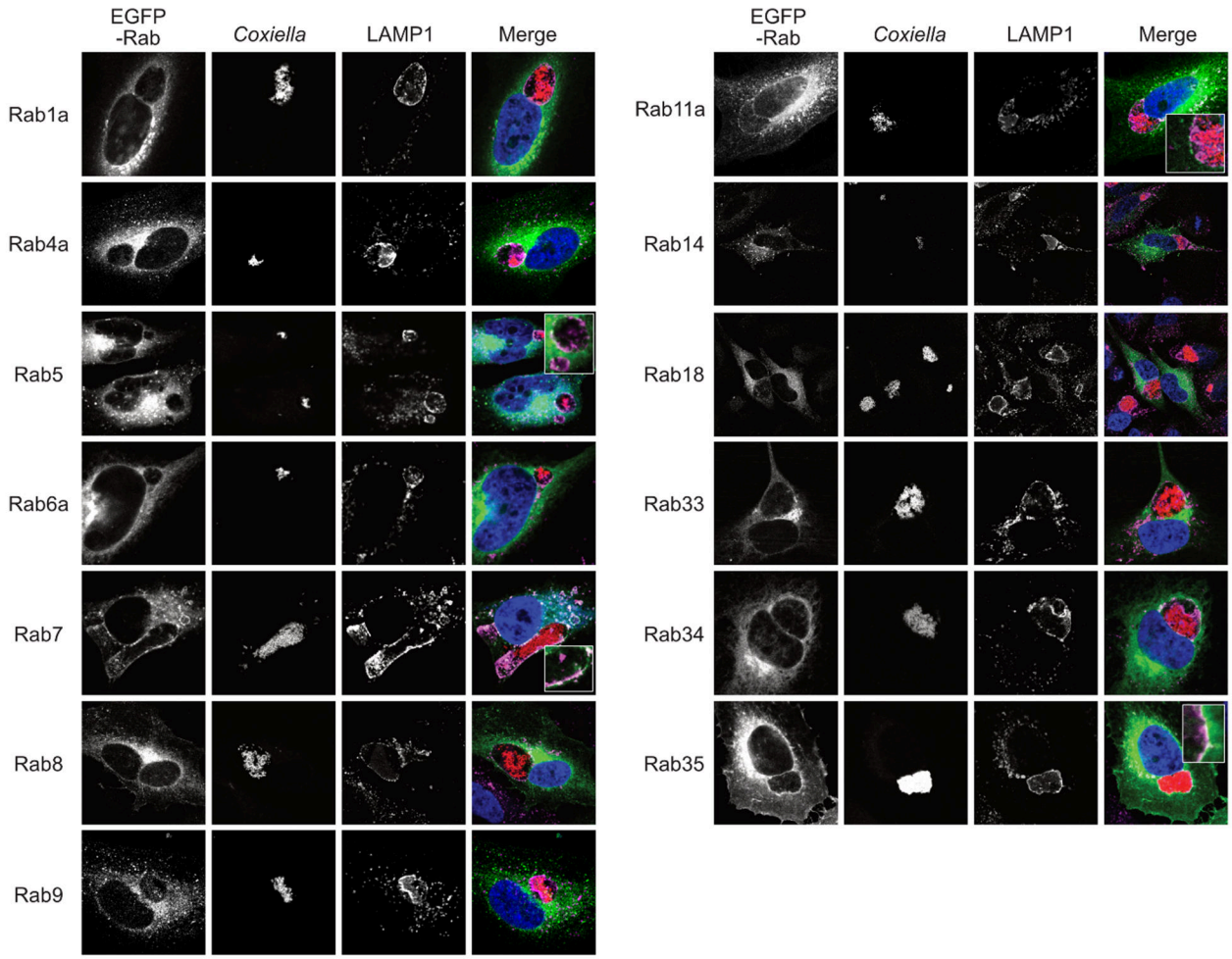

Figure 1. Host recycling endosome-associated proteins Rab11a and Rab35 localize to the CCV. Representative images of *Coxiella*-infected HeLa cells, expressing EGFP-tagged Rab proteins. HeLa cells were transfected with plasmids encoding EGFP-Rab proteins and at 24 h post-transfection, were infected with mCherry-*Coxiella* for 1 h. At 3 dpi, cells plated on coverslips were fixed and subjected to immunofluorescent assay with anti-LAMP1 antibody to label the CCVs. Cells were visualized with a Leica Stellaris confocal microscope and images were analyzed in ImageJ FIJI. CCVs, where LAMP1 and Rab proteins colocalized at the membrane (shown in insets) were considered positive for a specific Rab protein. As expected, CCVs were positive for both Rab5 and Rab7 at 3 dpi. Additionally, we observed that Rab11a and Rab35 also localized to CCVs. Notably, only a subset of CCVs were positive for Rab11a or Rab35.

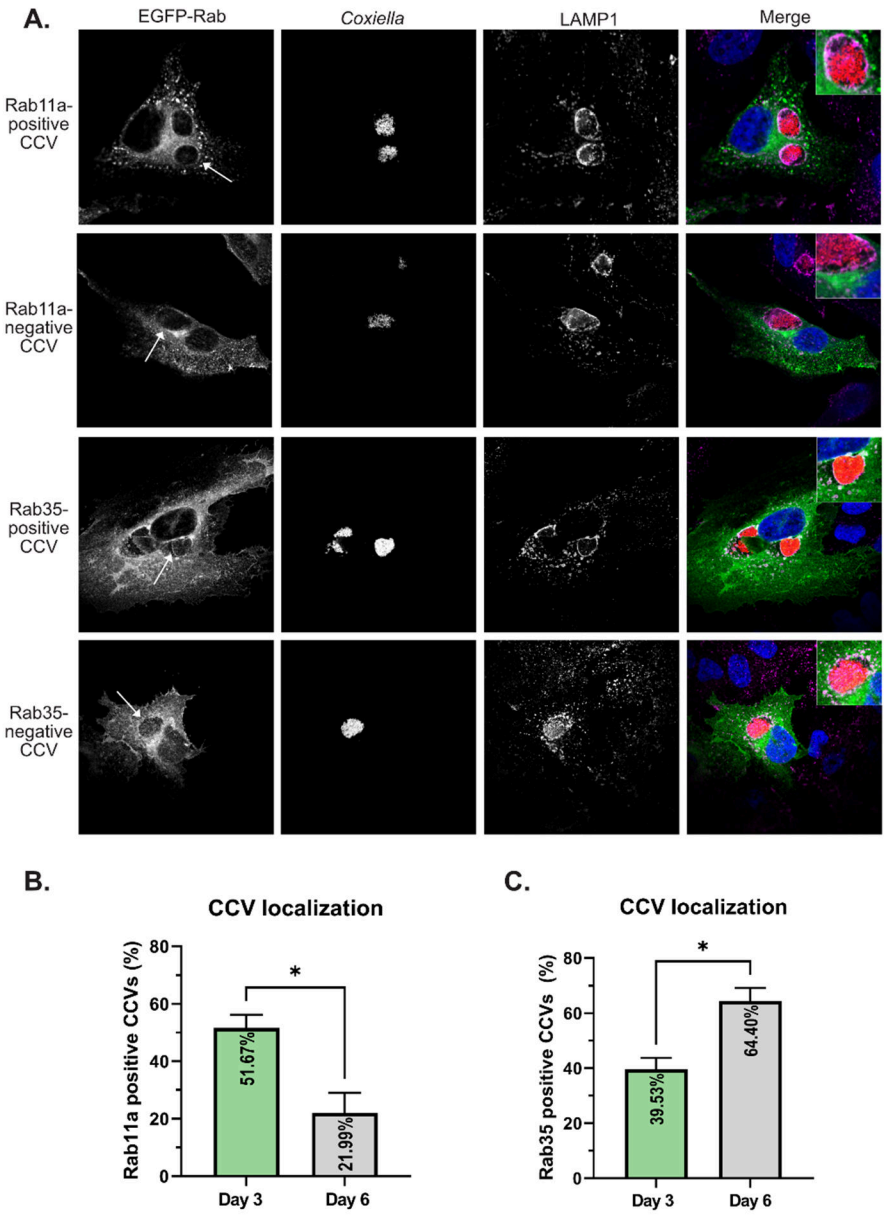

Figure 2. CCV-Rab11a and CCV-Rab35 interactions are dynamic and temporally regulated. (A) Representative images showing Rab11a and Rab35-positive and negative CCVs. HeLa cells were transfected with plasmids encoding EGFP-Rab11a or EGFP-Rab35 and at 24 h post-transfection, were infected with mCherry-*Coxiella* for 1 h. At 3 dpi, cells plated on coverslips were fixed and subjected to immunofluorescent assay with anti-LAMP1 antibody to label the CCVs. Cells were visualized with a Leica Stellaris confocal microscope and images were analyzed in ImageJ FIJI. CCVs, where LAMP1 and Rab proteins colocalized at the membrane (shown in insets) were considered positive for a specific Rab protein. CCVs were scored for Rab11a or Rab35 localization and percentage of positive CCVs were calculated. **(B-C)** Quantification of Rab11a- and Rab35-positive and negative CCVs at 3 and 6 dpi revealed that Rab11a localized to significantly more CCVs at 3 dpi compared to 6 dpi, whereas the pattern reversed for Rab35, which localized to more CCVs at 6 dpi. Data shown as mean±SEM of at least 100 infected cells per condition in each of three independent experiments (N=3) as analyzed by Welch's t-test; *, $P<0.05$.

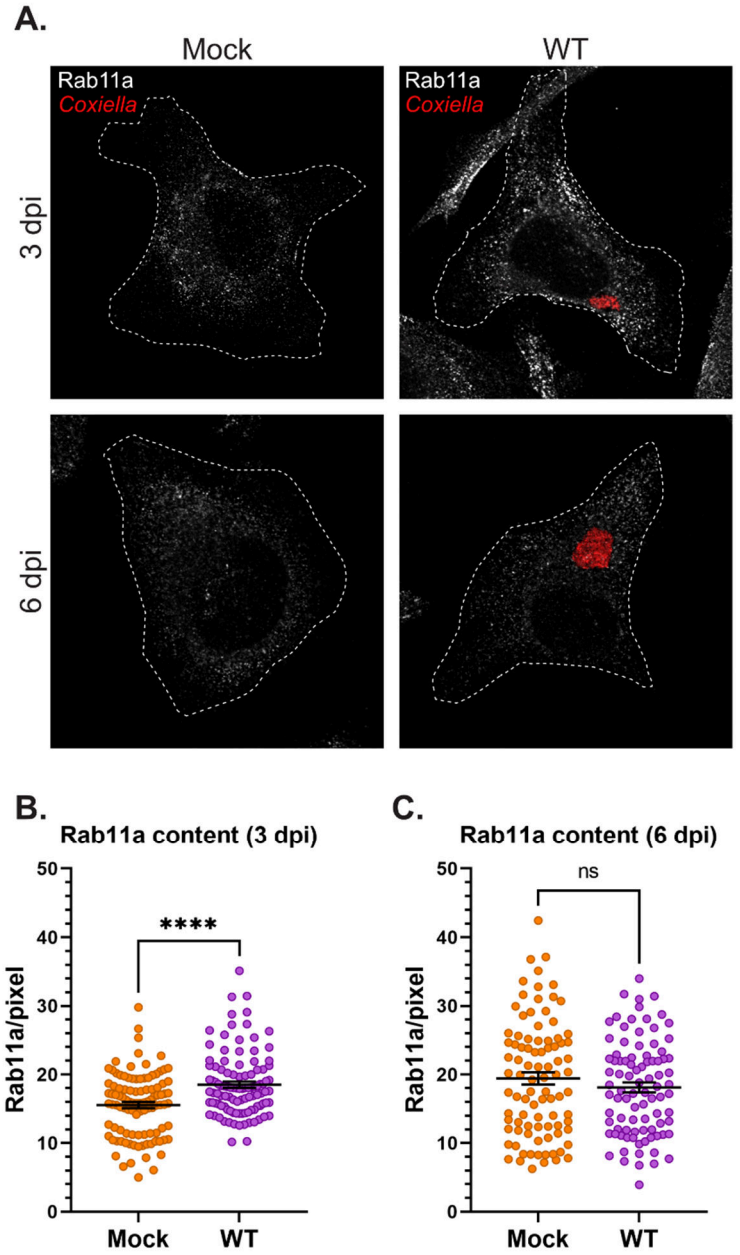

Figure 3. *Coxiella* increases Rab11a content in infected host cells. (A) Representative images showing Rab11a-positive recycling endosome content of mock and *Coxiella*-infected HeLa cells at 3 and 6 dpi. HeLa cells were mock infected or infected with mCherry-*Coxiella* for 1 h. On the days before the indicated time points, the cells were plated on coverslips. The next day, cells were fixed and subjected to immunofluorescent assay with anti-Rab11a antibody to uniformly stain the Rab11a-positive recycling endosomes. Cells were visualized with a Leica Stellaris confocal microscope and the images were analyzed in ImageJ FIJI. Identically captured images were imported into ImageJ FIJI and the total fluorescent intensity of Rab11a was measured and normalized to cell area. **(B-C)** Quantification of Rab11a fluorescent intensity revealed an increase in Rab11a content in *Coxiella*-infected cells at 3 dpi but not at 6 dpi. Data shown as mean±SEM of at least 25 cells per condition in each of three independent experiments (N=3) as analyzed by Welch's t-test; ****, P<0.0001; ns, non-significant.

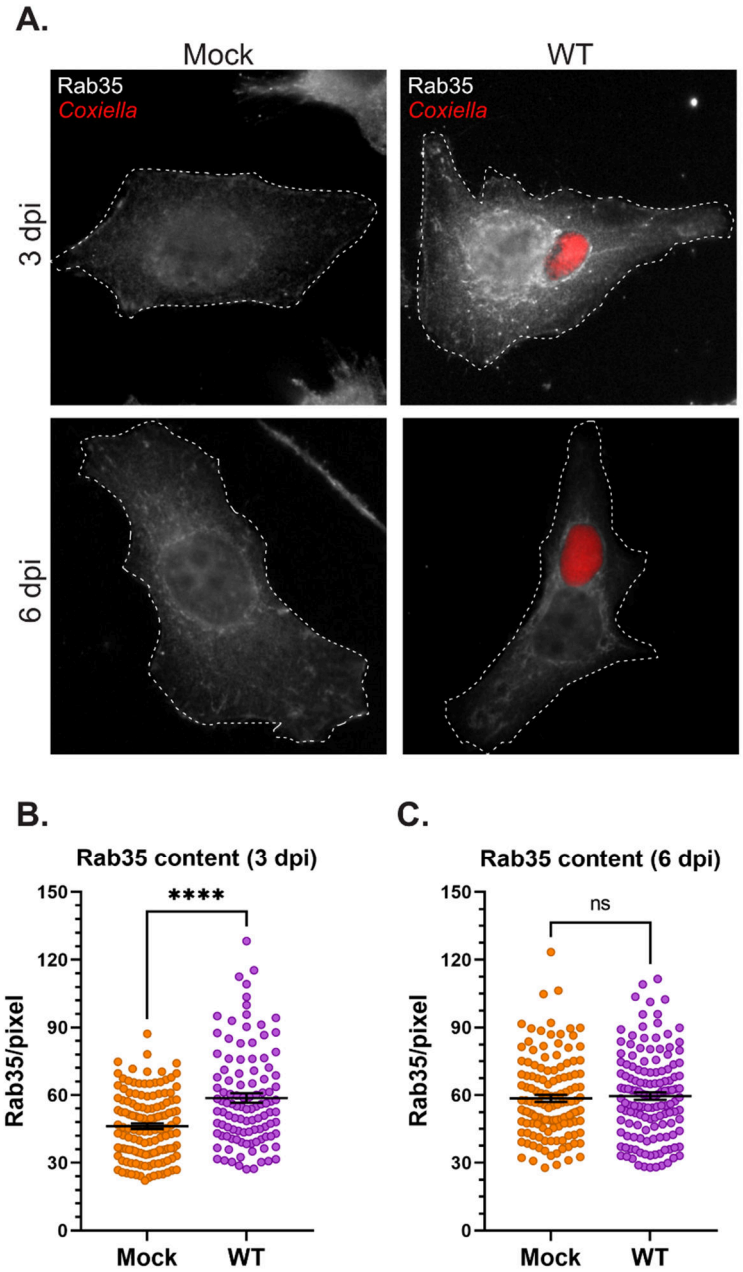

Figure 4. *Coxiella* increases Rab35 content in infected host cells. (A) Representative images showing Rab35-positive recycling endosome content of mock and *Coxiella*-infected HeLa cells at 3 and 6 dpi. HeLa cells were mock infected or infected with mCherry-*Coxiella* for 1 h. On the days before the indicated time points, the cells were plated on coverslips. The next day, cells were fixed and subjected to an immunofluorescent assay with anti-Rab35 antibody to uniformly stain the Rab35-positive recycling endosomes. Cells were visualized with a Leica Stellaris confocal microscope and the images were analyzed in ImageJ FIJI. Identically captured images were imported into ImageJ FIJI and the total fluorescent intensity of Rab35 was measured and normalized to cell area. **(B-C)** Quantification of Rab35 fluorescent intensity revealed an increase in Rab35 content in *Coxiella*-infected cells at 3 dpi but not at 6 dpi. Data shown as mean±SEM of at least 25 cells per condition in each of three independent experiments (N=3) as analyzed by Welch's t-test; ****, P<0.0001; ns, non-significant.

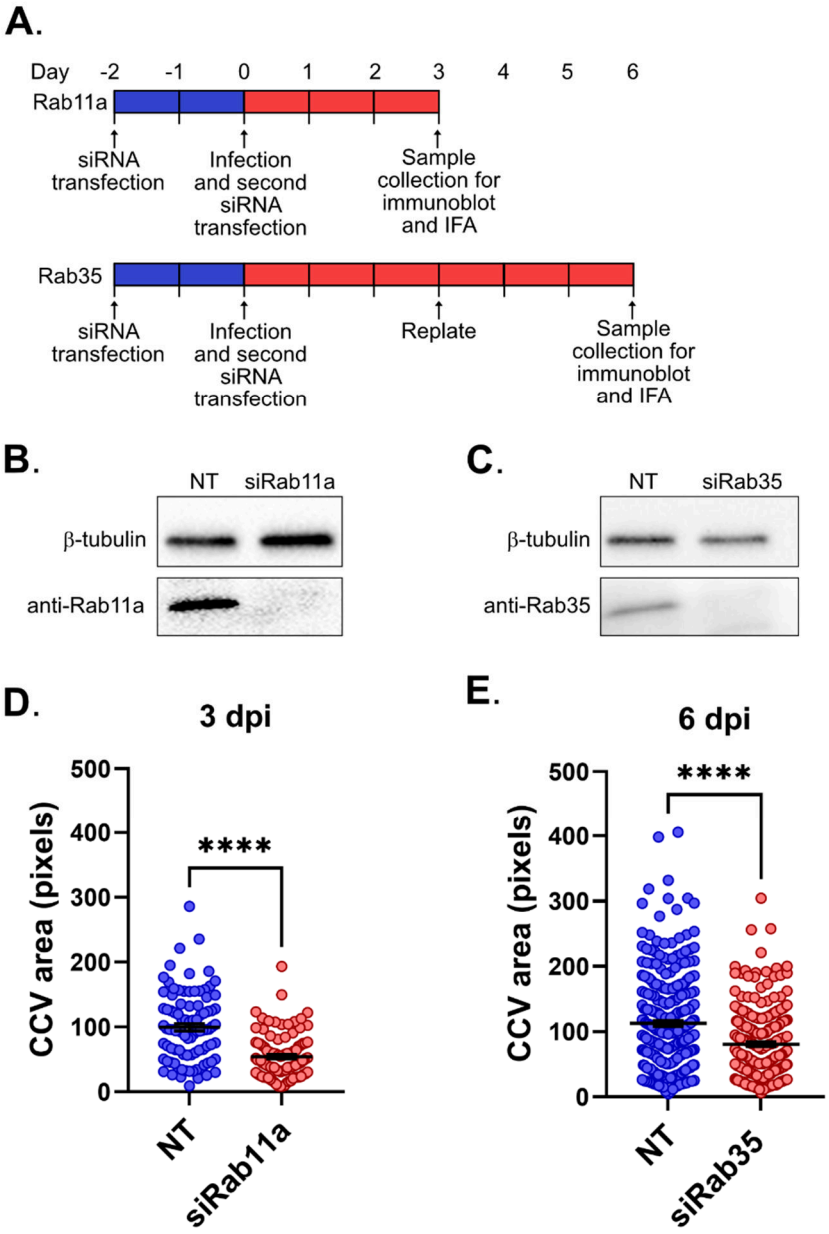

Figure 5. Rab11a and Rab35 are essential for CCV expansion. (A) Schematic diagram of dual siRNA transfection protocol in HeLa cells to silence Rab11a and Rab35. Cells were transfected with Rab11a or Rab35-specific siRNA (siRab11a or siRab35, respectively) or a control non-targeting siRNA (NT) and incubated. At 48 h post-transfection cells were infected with mCherry-*Coxiella* and subjected to a second round of siRNA transfection. At the indicated time points, cells were fixed and subjected to immunofluorescent assay with anti-LAMP1 antibody to label the CCVs. **(B-C)** Immunoblots revealed depletion of both Rab11a and Rab35 in siRNA-transfected cells at 3 and 6 dpi, respectively. **(D-E)** measurement of the CCV area revealed significantly smaller CCVs in siRab11a-transfected cells at 3 dpi and siRab35-transfected cells at 6 dpi. Data shown as mean±SEM of at least 25 cells per condition in each of three independent experiments (N=3) as analyzed by Welch's t-test; ****, $P<0.0001$; ns, non-significant.

460 **REFERENCES**
461

462 1. Maurin, M. and D. Raoult, *Q fever.* Clin Microbiol Rev, 1999. **12**(4): p. 518-53.

463 2. Eldin, C., et al., *Q fever in French Guiana.* Am J Trop Med Hyg, 2014. **91**(4): p. 771-6.

464 3. Angelakis, E., et al., *Coxiella burnetii-positive PCR in febrile patients in rural and urban*
465 *Africa.* Int J Infect Dis, 2014. **28**: p. 107-10.

466 4. White, B., T. Brooks, and R.A. Seaton, *Q fever in military and paramilitary personnel in*
467 *conflict zones: case report and review.* Travel Med Infect Dis, 2013. **11**(2): p. 134-7.

468 5. Amitai, Z., et al., *A large Q fever outbreak in an urban school in central Israel.* Clin Infect
469 Dis, 2010. **50**(11): p. 1433-8.

470 6. Porter, S.R., et al., *Q fever in Japan: an update review.* Vet Microbiol, 2011. **149**(3-4): p. 298-
471 306.

472 7. Lyytikainen, O., et al., *An outbreak of sheep-associated Q fever in a rural community in*
473 *Germany.* Eur J Epidemiol, 1998. **14**(2): p. 193-9.

474 8. Alonso, E., et al., *Q Fever Outbreak among Workers at a Waste-Sorting Plant.* PLoS One,
475 2015. **10**(9): p. e0138817.

476 9. Bjork, A., et al., *First reported multistate human Q fever outbreak in the United States, 2011.*
477 Vector Borne Zoonotic Dis, 2014. **14**(2): p. 111-7.

478 10. Nett, R.J., S.D. Helgerson, and A.D. Anderson, *Clinician assessment for Coxiella burnetii*
479 *infection in hospitalized patients with potentially compatible illnesses during Q fever*
480 *outbreaks and following a health alert, Montana, 2011.* Vector Borne Zoonotic Dis, 2013.
481 **13**(2): p. 128-30.

482 11. Graham, J.G., et al., *Development of an Ex Vivo Tissue Platform To Study the Human Lung*
483 *Response to Coxiella burnetii.* Infect Immun, 2016. **84**(5): p. 1438-1445.

484 12. Dragan, A.L., R.C. Kurten, and D.E. Voth, *Characterization of Early Stages of Human*
485 *Alveolar Infection by the Q Fever Agent Coxiella burnetii.* Infect Immun, 2019. **87**(5).

486 13. Howe, D. and L.P. Mallavia, *Coxiella burnetii exhibits morphological change and delays*
487 *phagolysosomal fusion after internalization by J774A.1 cells.* Infect Immun, 2000. **68**(7): p.
488 3815-21.

489 14. Voth, D.E. and R.A. Heinzen, *Lounging in a lysosome: the intracellular lifestyle of Coxiella*
490 *burnetii.* Cell Microbiol, 2007. **9**(4): p. 829-40.

491 15. Magunda, F., et al., *Anaplasma marginale actively modulates vacuolar maturation during*
492 *intracellular infection of its tick vector, Dermacentor andersoni.* Appl Environ Microbiol,
493 2016. **82**(15): p. 4715-4731.

494 16. Huang, B., et al., *The Anaplasma phagocytophilum-occupied vacuole selectively recruits Rab-*
495 *GTPases that are predominantly associated with recycling endosomes.* Cell Microbiol, 2010.
496 **12**(9): p. 1292-307.

497 17. Clemens, D.L. and M.A. Horwitz, *Characterization of the Mycobacterium tuberculosis*
498 *phagosome and evidence that phagosomal maturation is inhibited.* J Exp Med, 1995. **181**(1):
499 p. 257-70.

500 18. Horwitz, M.A., *The Legionnaires' disease bacterium (Legionella pneumophila) inhibits*
501 *phagosome-lysosome fusion in human monocytes.* J Exp Med, 1983. **158**(6): p. 2108-26.

502 19. Connor, M.G., et al., *Yersinia pestis Requires Host Rab1b for Survival in Macrophages.* PLoS
503 Pathog, 2015. **11**(10): p. e1005241.

504 20. Mulye, M., et al., *Elevated Cholesterol in the Coxiella burnetii Intracellular Niche Is*
505 *Bacteriolytic.* mBio, 2017. **8**(1).

506 21. Samanta, D., et al., *Coxiella burnetii Type 4B Secretion System-dependent manipulation of*
507 *endolysosomal maturation is required for bacterial growth.* PLoS Pathog, 2019. **15**(12): p.
508 e1007855.

509 22. Newton, H.J., J.A. McDonough, and C.R. Roy, *Effector protein translocation by the Coxiella*
510 *burnetii Dot/Icm type IV secretion system requires endocytic maturation of the pathogen-*
511 *occupied vacuole.* PLoS One, 2013. **8**(1): p. e54566.

512 23. Ghigo, E., M.I. Colombo, and R.A. Heinzen, *The Coxiella burnetii parasitophorous vacuole.*
513 Adv Exp Med Biol, 2012. **984**: p. 141-69.

514 24. Huotari, J. and A. Helenius, *Endosome maturation.* EMBO J, 2011. **30**(17): p. 3481-500.

515 25. Wandinger-Ness, A. and M. Zerial, *Rab proteins and the compartmentalization of the*
516 *endosomal system.* Cold Spring Harb Perspect Biol, 2014. **6**(11): p. a022616.

517 26. Beare, P.A., et al., *Characterization of a Coxiella burnetii ftsZ mutant generated by Himar1*
518 *transposon mutagenesis.* J Bacteriol, 2009. **191**(5): p. 1369-81.

519 27. Coleman, S.A., et al., *Temporal analysis of Coxiella burnetii morphological differentiation.* J
520 Bacteriol, 2004. **186**(21): p. 7344-52.

521 28. Faris, R., et al., *Chlamydia trachomatis CT229 Subverts Rab GTPase-Dependent CCV*
522 *Trafficking Pathways to Promote Chlamydial Infection.* Cell Rep, 2019. **26**(12): p. 3380-3390
523 e5.

524 29. Schindelin, J., et al., *Fiji: an open-source platform for biological-image analysis.* Nat
525 Methods, 2012. **9**(7): p. 676-82.

526 30. Beron, W., et al., *Coxiella burnetii localizes in a Rab7-labeled compartment with autophagic*
527 *characteristics.* Infect Immun, 2002. **70**(10): p. 5816-21.

528 31. Romano, P.S., et al., *The autophagic pathway is actively modulated by phase II Coxiella*
529 *burnetii to efficiently replicate in the host cell.* Cell Microbiol, 2007. **9**(4): p. 891-909.

530 32. Chaineau, M., M.S. Ioannou, and P.S. McPherson, *Rab35: GEFs, GAPs and effectors.* Traffic,
531 2013. **14**(11): p. 1109-17.

532 33. Grant, B.D. and J.G. Donaldson, *Pathways and mechanisms of endocytic recycling.* Nat Rev
533 Mol Cell Biol, 2009. **10**(9): p. 597-608.

534 34. Ullrich, O., et al., *Rab11 regulates recycling through the pericentriolar recycling endosome.* J
535 Cell Biol, 1996. **135**(4): p. 913-24.

536 35. Plutner, H., et al., *Rab1b regulates vesicular transport between the endoplasmic reticulum*
537 *and successive Golgi compartments.* J Cell Biol, 1991. **115**(1): p. 31-43.

538 36. van der Sluijs, P., et al., *The small GTP-binding protein rab4 controls an early sorting event*
539 *on the endocytic pathway.* Cell, 1992. **70**(5): p. 729-40.

540 37. Chavrier, P., et al., *Localization of low molecular weight GTP binding proteins to exocytic*
541 *and endocytic compartments.* Cell, 1990. **62**(2): p. 317-29.

542 38. Goud, B., et al., *Small GTP-binding protein associated with Golgi cisternae.* Nature, 1990.
543 **345**(6275): p. 553-6.

544 39. Huber, L.A., et al., *Rab8, a small GTPase involved in vesicular traffic between the TGN and*
545 *the basolateral plasma membrane.* J Cell Biol, 1993. **123**(1): p. 35-45.

546 40. Yoshimura, S., et al., *Functional dissection of Rab GTPases involved in primary cilium*
547 *formation.* J Cell Biol, 2007. **178**(3): p. 363-9.

548 41. Ren, M., et al., *Hydrolysis of GTP on rab11 is required for the direct delivery of transferrin*
549 *from the pericentriolar recycling compartment to the cell surface but not from sorting*
550 *endosomes.* Proc Natl Acad Sci U S A, 1998. **95**(11): p. 6187-92.

551 42. Junutula, J.R., et al., *Rab14 is involved in membrane trafficking between the Golgi complex*
552 *and endosomes.* Mol Biol Cell, 2004. **15**(5): p. 2218-29.

553 43. Dejgaard, S.Y., et al., *Rab18 and Rab43 have key roles in ER-Golgi trafficking.* J Cell Sci,
554 2008. **121**(Pt 16): p. 2768-81.

555 44. Zheng, J.Y., et al., *A novel Rab GTPase, Rab33B, is ubiquitously expressed and localized to*
556 *the medial Golgi cisternae.* J Cell Sci, 1998. **111 (Pt 8)**: p. 1061-9.

557 45. Wang, T. and W. Hong, *Interorganellar regulation of lysosome positioning by the Golgi*
558 *apparatus through Rab34 interaction with Rab-interacting lysosomal protein.* Mol Biol Cell,
559 2002. **13**(12): p. 4317-32.

560 46. Kouranti, I., et al., *Rab35 regulates an endocytic recycling pathway essential for the terminal*
561 *steps of cytokinesis.* Curr Biol, 2006. **16**(17): p. 1719-25.

562 47. O'Sullivan, M.J. and A.J. Lindsay, *The Endosomal Recycling Pathway-At the Crossroads of*
563 *the Cell.* Int J Mol Sci, 2020. **21**(17).

564 48. Hopkins, C.R. and I.S. Trowbridge, *Internalization and processing of transferrin and the*
565 *transferrin receptor in human carcinoma A431 cells.* J Cell Biol, 1983. **97**(2): p. 508-21.

566 49. Allgood, S.C. and M.R. Neunuebel, *The recycling endosome and bacterial pathogens.* Cell
567 Microbiol, 2018. **20**(7): p. e12857.

568 50. Green, E.G., et al., *Rab11 is associated with transferrin-containing recycling compartments in*
569 *K562 cells.* Biochem Biophys Res Commun, 1997. **239**(2): p. 612-6.

570 51. Molleken, K. and J.H. Hegemann, *Acquisition of Rab11 and Rab11-Fip2-A novel strategy for*
571 *Chlamydia pneumoniae early survival.* PLoS Pathog, 2017. **13**(8): p. e1006556.

572 52. Baetz, N.W. and J.R. Goldenring, *Rab11-family interacting proteins define spatially and*
573 *temporally distinct regions within the dynamic Rab11a-dependent recycling system.* Mol Biol
574 Cell, 2013. **24**(5): p. 643-58.

575 53. Leiva, N., A. Capmany, and M.T. Damiani, *Rab11-family of interacting protein 2 associates*
576 *with chlamydial inclusions through its Rab-binding domain and promotes bacterial*
577 *multiplication.* Cell Microbiol, 2013. **15**(1): p. 114-29.

578 54. Rejman Lipinski, A., et al., *Rab6 and Rab11 regulate Chlamydia trachomatis development*
579 *and golgin-84-dependent Golgi fragmentation.* PLoS Pathog, 2009. **5**(10): p. e1000615.

580 55. Ouellette, S.P. and R.A. Carabeo, *A Functional Slow Recycling Pathway of Transferrin is*
581 *Required for Growth of Chlamydia.* Front Microbiol, 2010. **1**: p. 112.

582 56. Larson, C.L. and R.A. Heinzen, *High-Content Imaging Reveals Expansion of the Endosomal*
583 *Compartment during Coxiella burnetii Parasitophorous Vacuole Maturation.* Front Cell
584 Infect Microbiol, 2017. **7**: p. 48.

585 57. Allgood, S.C., et al., *Legionella Effector AnkX Disrupts Host Cell Endocytic Recycling in a*
586 *Phosphocholination-Dependent Manner.* Front Cell Infect Microbiol, 2017. **7**: p. 397.

587 58. Howe, D., et al., *Maturation of the Coxiella burnetii parasitophorous vacuole requires*
588 *bacterial protein synthesis but not replication.* Cell Microbiol, 2003. **5**(7): p. 469-80.

589 59. Ryan, T.A., *Kiss-and-run, fuse-pinch-and-linger, fuse-and-collapse: the life and times of a*
590 *neurosecretory granule.* Proc Natl Acad Sci U S A, 2003. **100**(5): p. 2171-3.

591 60. Zulkefli, K.L., et al., *A role for Rab11 in the homeostasis of the endosome-lysosomal pathway.*
592 Exp Cell Res, 2019. **380**(1): p. 55-68.

593